Published online 24 December 2021

Nucleic Acids Research, 2022, Vol. 50, No. 3 ***1269–1279***
https://doi.org/10.1093/nar/gkab1252

DNA supercoiling-mediated collective behavior of co-transcribing RNA polymerases

Shubham Tripathi [1,2], Sumitabha Brahmachari[3], José N. Onuchic[3,4] and Herbert Levine[2,*]

[1]PhD Program in Systems, Synthetic, and Physical Biology, Rice University, Houston, TX, USA, [2]Center for Theoretical Biological Physics & Department of Physics, Northeastern University, Boston, MA, USA, [3]Center for Theoretical Biological Physics, Rice University, Houston, TX, USA and [4]Department of Physics and Astronomy, Department of Chemistry, & Department of Biosciences, Rice University, Houston, TX, USA

Received April 29, 2021; Revised December 02, 2021; Editorial Decision December 03, 2021; Accepted December 06, 2021

ABSTRACT

Multiple RNA polymerases (RNAPs) transcribing a gene have been known to exhibit collective group behavior, causing the transcription elongation rate to increase with the rate of transcription initiation. Such behavior has long been believed to be driven by a physical interaction or 'push' between closely spaced RNAPs. However, recent studies have posited that RNAPs separated by longer distances may cooperate by modifying the DNA segment under transcription. Here, we present a theoretical model incorporating the mechanical coupling between RNAP translocation and the DNA torsional response. Using stochastic simulations, we demonstrate DNA supercoiling-mediated long-range cooperation between co-transcribing RNAPs. We find that inhibiting transcription initiation can slow down the already recruited RNAPs, in agreement with recent experimental observations, and predict that the average transcription elongation rate varies non-monotonically with the rate of transcription initiation. We further show that while RNAPs transcribing neighboring genes oriented in tandem can cooperate, those transcribing genes in divergent or convergent orientations can act antagonistically, and that such behavior holds over a large range of intergenic separations. Our model makes testable predictions, revealing how the mechanical interplay between RNAPs and the DNA they transcribe can govern transcriptional dynamics.

INTRODUCTION

Genomic DNA is double-stranded, with the two strands wrapped helically around one another. The topology of DNA imposes a constraint on the movement of RNA polymerases (RNAPs) along the DNA during transcription, first conceptualized in the twin supercoiled domain model (1). The model postulated that transcription would result in overtwisting of the DNA downstream from the RNAP (positive supercoiling) and undertwisting of the DNA upstream from the RNAP (negative supercoiling). Recent experimental studies have described a role for transcription-associated DNA supercoiling in many biological processes, such as transcriptional bursting (2), control of transcription elongation (3), and formation of chromosomal domains in bacteria (4–6) and eukaryotes (7–9). Simultaneously, single-molecule experiments have shed light on how molecular motors like RNAPs respond to mechanical interventions including DNA stretching and twisting (10,11). Together, these experimental advances have resulted in both a need and an opportunity for the development of a theoretical framework of the transcription-supercoiling interplay (12–18) that can help with the analysis of the existing experimental data and make testable predictions to guide future study design.

Transcription in prokaryotes involves two distinct steps—transcription initiation and transcription elongation. During transcription initiation, an RNAP is recruited to the gene promoter. The two DNA strands are then locally separated by the RNAP to form a transcription bubble (19). During transcription elongation, the bubble translocates along the gene body. Previous studies have suggested that multiple RNAPs co-transcribing a gene can cooperate via physical collisions between adjacent RNAPs (12,20–22). However, recent experiments suggest that DNA torsion or supercoiling can mediate long-distance interaction among co-transcribing RNAPs (3). These observations have sparked interest in the possibility of a physical model of co-transcribing RNAPs that can re-capitulate the reported behavior if the RNAPs interact only via the DNA under transcription.

In the present study, we build upon the well-known biophysical properties of DNA as a polymer (23–26) and of RNAP translocation (10) to describe a theoretical model of the transcription-supercoiling interplay. In our model, RNAP translocation on topologically constrained DNA

*To whom correspondence should be addressed. Tel: +1 858 395 8261; Email: h.levine@northeastern.edu

generates negative supercoiling upstream of the RNAP and positive supercoiling downstream of the RNAP, along with corresponding DNA torques. Co-transcribing RNAPs in our model interact via this RNAP-generated DNA torque. We hypothesize, based on single-molecule experiments (10), that a net positive torque difference between the front and the back of a transcribing RNAP is a repressor of transcription elongation. With model parameters in the biophysical range, we find that neutralization of DNA twist by co-transcribing RNAPs can lead to a regime of collective behavior with transcription elongation rates higher than that for the case of a single transcribing RNAP. Furthermore, we show that transcription-generated DNA supercoiling can drive coupling between co-transcribing RNAPs separated by long distances, including those transcribing neighboring genes. Clearly, such long-distance interaction is incompatible with a purely physical 'push'-based interaction between closely spaced RNAPs (20–22). We further investigated the model behavior under varying gene lengths and the relative orientation of neighboring genes, and explored how transcription elongation is affected by biological processes such as DNA topological relaxation and maintenance of DNA in a twisted state. Our model interprets existing experimental results in the light of the DNA supercoiling-transcription interplay, and makes testable predictions.

MATERIALS AND METHODS

A theoretical model of DNA supercoiling-transcription elongation interplay

During transcription elongation, the transcription bubble translocates along the DNA, requiring the RNAP to track the DNA helical groove. This can be accomplished via rotation of the RNAP around the axis of the DNA double helix or DNA twisting. When an RNAP translocates over a distance x nm, there is accumulation of a rotational angle $\omega_0 x$ due to the helically linked structure of the DNA. Here, $\omega_0 = 1.85\ \text{nm}^{-1}$ is the linking number density in unstressed double-stranded DNA (27). If the DNA is torsionally constrained (for example, by DNA-binding proteins (28,29)), the accumulated rotational angle is conserved and is partitioned between the rotation angle of the RNAP (θ) and the DNA rotation at the RNAP site, or DNA twist (ϕ) (Figure 1A). We write the linking number constraint, or partition equation:

$$\omega_0 x = \theta + \phi \tag{1}$$

While RNAP rotation is opposed by the viscous, or hydrodynamic, drag on the RNAP-nascent RNA complex, DNA rotation at the RNAP site is opposed by the restoring torque arising from the twisting of the torsionally constrained DNA. Note that since translation occurs simultaneously with transcription in prokaryotes, the RNAP-nascent RNA complex will include the translation machinery. The balance between the viscous drag and the DNA restoring torque during RNAP translocation thus dictates the partitioning of the accumulated rotational angle between RNAP rotation and DNA twist. Following Sevier and Levine (14), we write the torque-balance equation in the regime of overdamped dynamics:

$$\chi \frac{d\phi}{dt} = \eta x^{\alpha} \frac{d\theta}{dt} - (\tau_f - \tau_b) \tag{2}$$

Here, χ is the DNA twist mobility. The first term on the right hand side of Equation (2) describes the rotational viscous drag on the RNAP complex which grows with an increase in the nascent RNA length (equal to x), the growth rate dictated by the exponent α. This drag is also dependent on the coefficient of friction η and the rotational velocity of the RNAP complex ($\frac{d\theta}{dt}$). The different parameters were chosen to be within the biophysical range based on experimental data (Appendix Sec. 1 and (30)).

The second term on the right hand side in Equation (2) describes the net DNA restoring torque, equal to the difference between the torques applied by the DNA segments downstream and upstream from the RNAP (τ_f and τ_b, respectively). The DNA restoring torque is a function of the excess linking number density, or the DNA supercoiling density σ, and was calculated as described previously (23–25) (see Eqs. (S2) and (S3), Supplementary Figures S1 and S2). The restoring torque depends linearly on σ in regimes where supercoiling increases the DNA twist. When σ is higher than a critical linking number density (24), the torque exceeds the critical buckling torque. Consequently, the DNA buckles, leading to the coexistence of plectonemes and twisted DNA. In this buckled regime, increasing σ causes higher plectoneme writhe, while DNA twist and the corresponding DNA restoring torque remain constant. In the negative supercoiling regime, torques exceeding $\approx$10 pN·nm or $2.5 k_B T$ in magnitude destabilize the right-handed DNA helix resulting in the melting of DNA base pairs (note that the average base-pairing energy is $\approx 2 k_B T$ per base pair) (10,23,25). Melted DNA is extremely floppy to twisting (as well as bending) deformations, and can easily accommodate additional twist without an appreciable change in the DNA restoring torque (23,25,26). Coexistence of this floppy melted DNA state along with twisted DNA leads to a torque plateau in the negative supercoiling regime (Supplementary Figure S1).

Note that the equations describing the σ−torque relation (Eq. S3) employed here were derived using a free energy that is harmonic in σ (23,25). These equations are applicable to bulk thermodynamic systems and the DNA behavior shows deviations in finite-size systems (24,31). For example, when the DNA segment between two adjacent RNAPs is very small ($\approx$100 nm), the bulk thermodynamics framework underestimates the critical supercoiling density at which the DNA can start forming plectonemes. In the present study, we have used a phenomenological correction factor to avoid the unphysical scenario wherein DNA segments of the order of the DNA persistence length form plectonemes (see Appendix Sec. 2 and Supplementary Figure S2 for details). Finally, as shown in Supplementary Figure S1, the DNA torsional response also depends on the DNA stretching force. In an *in vivo* setting, the genomic DNA can experience stretching forces owing to multiple effects, including the entropic degrees of freedom of DNA as a polymer, osmotic repulsion arising from self-avoidance, and the dynamics of DNA-binding proteins (27). In an *in vitro* single-molecule setup, the DNA stretching force can be

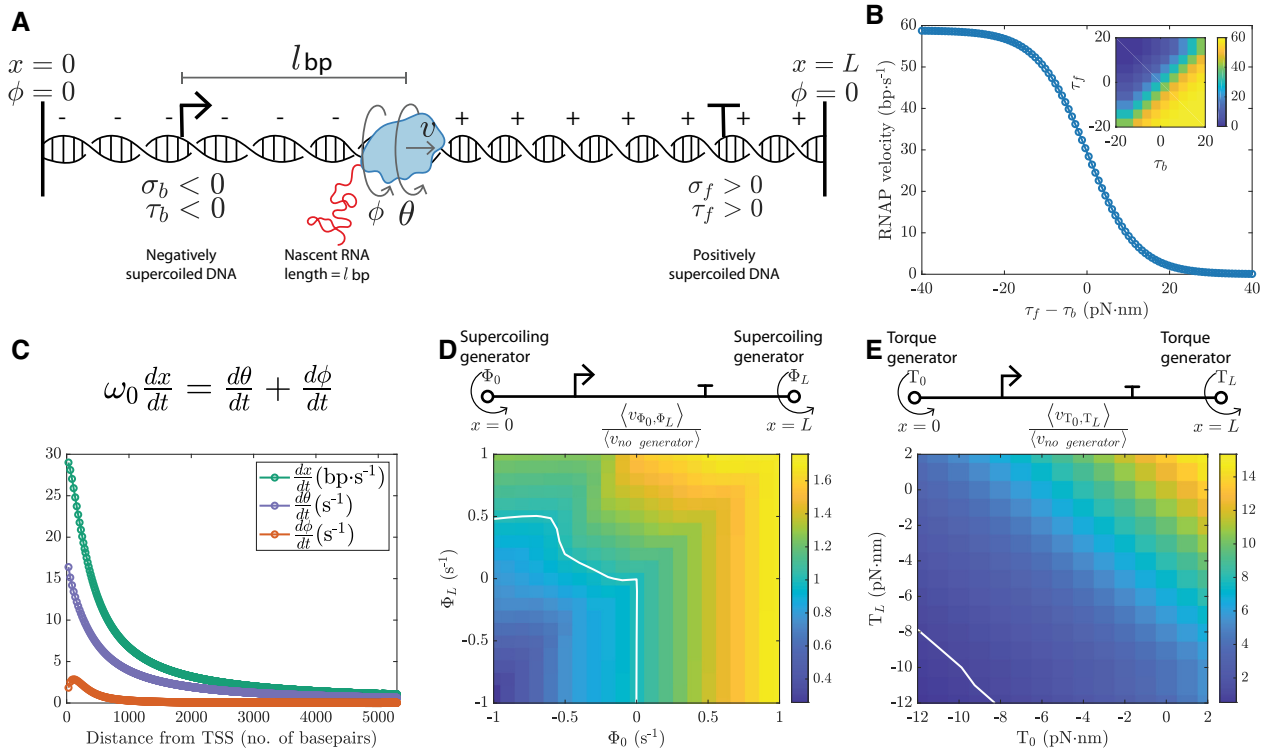

Figure 1. Mechanical coupling between RNAP translocation and the DNA torsional response. (**A**) RNAP translocation on a torsionally constrained DNA segment is accompanied by undertwisting of the DNA upstream ($\sigma_b < 0$) and overtwisting of the DNA downstream ($\sigma_f > 0$). The supercoiled DNA, in turn, applies a restoring torque on the RNAP (τ_b and τ_f). (**B**) In agreement with the experimental data (10), we used a sigmoid curve (Equation 3) to model the RNAP velocity-DNA restoring torque dependence. (**C**) As the RNAP moves away from the transcription start site (TSS), its translocation rate ($\frac{dx}{dt}$) and rotation rate ($\frac{d\theta}{dt}$) continuously decreases, while the rate of DNA twisting by the RNAP ($\frac{d\phi}{dt}$) exhibits a non-monotonic trend. The behavior shown here is for the case of a torsionally constrained genomic segment. (**D**) Ratio of the average RNAP velocity in the presence of different supercoiling generators to the average RNAP velocity in the absence of any supercoiling generators. Here, Φ_0 and Φ_L are the rates of supercoiling injection upstream and downstream from the gene body, respectively. See Eqs. (S5) and (S6) for further details. (**E**) Ratio of the average RNAP velocity in the presence of different torque generators to the average RNAP velocity in the absence of any torque generators. Here, T_0 and T_L are the torques applied by an external agent or process upstream and downstream from the gene body, respectively. See Eqs. (S7) and (S8) for further details. In (D) and (E), the white line demarcates the region where the average RNAP velocity is lower in the presence of the generators from the region where the presence of generators increases the average RNAP velocity. The average RNAP velocity is defined as the gene length divided by the total time taken by the RNAP to transcribe the gene.

controlled via a magnetic bead attached to one end of the DNA segment or via optical tweezers (32). In the present study, we have investigated the model behavior for a stretching force of 1 pN.

Experiments have shown that the RNAP translocation rate, or RNAP velocity ($\frac{dx}{dt}$), also depends on the DNA torsional stress. Based on experimental observations (10), we used a sigmoid curve to model this dependence (Figure 1B):

$$\frac{dx}{dt} \equiv v = \left(\frac{v_0}{2}\right)\left(1 - \tanh\left(\frac{\tau_f - \tau_b}{\tau_c}\right)\right) \qquad (3)$$

Here, $v_0 = 20$ nm·s^{-1} ≈ 60 bp·s^{-1} is the maximum RNAP velocity. Note that when the restoring torques in the front and back of the RNAP are the same, *i.e.*, the net restoring torque is zero, the RNAP velocity is $\frac{v_0}{2}$. RNAPs stall if $\tau_f - \tau_b > \tau_c = 12$ pN·nm. Thus, both positive torque downstream and negative torque upstream can stall an RNAP. If the net DNA restoring torque is negative ($\tau_f < \tau_b$), the DNA torsional response does not impede RNAP movement since in this scenario, RNAP translocation will twist the DNA to a more relaxed configuration. If the net restoring torque is positive ($\tau_f > \tau_b$), the DNA torsional response hinders RNAP movement since now the RNAP must further increase the DNA torsional stress in order to translocate.

We used the theoretical framework described by Equations (1)–(3) both to simulate the behavior of a single RNAP under different mechanical interventions and to probe how multiple RNAPs co-transcribing the same gene or neighboring genes will interact (see Supplementary Figure S3 for the different simulation setups). Unless otherwise stated, the gene length in our simulations is 5.3 kb (kilo base pairs) which is equal to the length of the *lac* operon in *Escherichia coli*. Both the model setup and the model parameters were chosen to capture the transcription behavior in prokaryotes. While the basic framework of DNA supercoiling-mediated coupling between RNAPs described here will be applicable to eukaryotes as well, the behavior is likely to be far more complex due to the presence of nucleosomes and other factors (33). Some of the changes that will be required to adapt the present model to describe transcription in eukaryotes are described in Appendix Sec. 3.

RESULTS

A transcribing RNAP continually slows down due to the accumulated DNA torsional stress

Starting with a single RNAP at the transcription start site (TSS), the dynamical system defined by Equations (2) and (3) can be integrated numerically, under the linking number constraint in Equation (1), to obtain the deterministic velocity profile of the RNAP. For a single transcribing RNAP, the instantaneous velocity decreases monotonically as the RNAP translocates along the gene body (Figure 1C). This slowdown is a direct consequence of the accumulation of transcription-generated DNA supercoiling (positive supercoiling downstream and negative supercoiling upstream of the RNAP), leading to higher DNA torque opposing RNAP movement. At the transcription start site, the net DNA restoring torque opposing RNAP movement is zero, and the instantaneous RNAP velocity is $\frac{v_0}{2} \approx 30$ bp·s^{-1} (Equation 3). Transcription elongation away from the TSS involves both RNAP rotation and DNA twisting in order to accommodate the DNA linking number. The angular velocity of RNAP rotation ($\frac{d\theta}{dt}$) decays monotonically due to the increasing viscous drag on the RNAP complex as the nascent RNA elongates (Figure 1C). The rate of DNA twisting ($\frac{d\phi}{dt}$), in contrast, increases initially with RNAP translocation to compensate for the slowdown in the RNAP rotation rate. However, with the consequent increase in the DNA restoring torque, the DNA rotation soon starts decreasing and the decrease continues with further RNAP translocation along the gene body (Figure 1C). In contrast, in the case of a torsionally unconstrained genomic segment, there is no DNA restoring torque on the RNAP since the DNA twist can simply diffuse out from the free DNA ends. Consequently, the rate of DNA rotation increases monotonically and the RNAP velocity remains constant as it translocates along the gene body (Supplementary Figure S4). While changing the DNA stretching force can alter the DNA twisting profile, it has little effect on the RNAP velocity (Supplementary Figure S5).

Note that in Figure 1C, we fixed the DNA boundaries, imposing a fixed overall DNA linking number on the DNA segment under consideration. Instead, DNA twist can be injected into a genomic section from the boundaries by a biological process or by an external agent. In single-molecule studies, magnetic tweezers are used to characterize the DNA's response to twist injection. In cells, enzymes such as topoisomerases inject negative and positive supercoiling into the DNA (34–36). Both DNA transcription and replication machineries (37) can inject supercoiling into the neighboring DNA. We analyzed the RNAP velocity in the presence of supercoiling generators (Figure 1D), which inject supercoiling at a constant rate, and torque generators (Figure 1E), which inject supercoiling until the restoring torque in the DNA segment reaches a constant value (T_0 or T_L in Figure 1E). In Figure 1D, the generator at $x = 0$ injects positive supercoiling upstream of the RNAP for $\Phi_0 > 0$. The generator at $x = L$ injects negative supercoiling downstream of the RNAP for $\Phi_L > 0$. The generators-injected supercoiling can cancel out the RNAP-generated supercoiling, resulting in higher average transcription elongation rate for larger, positive values of Φ_0 and Φ_L. In contrast, for Φ_0, $\Phi_L < 0$, negative supercoiling is injected upstream of the RNAP and positive supercoiling is injected downstream of the RNAP. This adds to the RNAP-generated supercoiling, thereby slowing down the RNAP. In Figure 1E, we report similar behavior: higher average RNAP velocity for higher values of T_0 and T_L which once again arises from the cancellation of the RNAP-generated supercoiling. Note that while setting $\Phi_0 = \Phi_L = 0$ results in the baseline case of absence of any supercoiling generators at the ends of the genomic segment, setting $T_0 = T_L = 0$ does not automatically result in baseline behavior. Consequently, the white contour corresponding to no change in average RNAP velocity as compared to the baseline is close to $\Phi_0 = \Phi_L = 0$ in Figure 1D but not close to $T_0 = T_L = 0$ in Figure 1E. Together, Figure 1D–E shows that DNA twisting by an external process can affect translocation of an RNAP. The case when the DNA twisting comes from the other co-transcribing RNAPs is described next.

Emergence of collective RNAP behavior: recruitment of new RNAPs speeds up the already transcribing RNAPs

To explore how multiple RNAPs co-transcribing a gene may interact, we incorporated two stochastic processes into our modeling framework—recruitment of RNAPs to the TSS at a rate k_{on} and global relaxation of the DNA supercoiling density to its basal value $\sigma_{basal} = 0$ at a rate k_{relax} (Figure 2A). The transcription initiation rate k_{on} is supercoiling density-independent in the present study and is kept unchanged during the simulation run. Using the Gillespie algorithm (38) to simulate stochastic model behavior, we find that the recruitment of additional RNAPs to the TSS speeds up the already transcribing RNAPs (Figure 2B). Such behavior arises from the cancellation of the negative supercoiling injected by the leading RNAP into the upstream DNA by the positive supercoiling injected by the newly recruited RNAP into the same DNA segment. This cancellation reduces the net DNA restoring torque on the leading RNAP, increasing its translocation speed (Supplementary Figure S6). The coupling between co-transcribing RNAPs disappears if the DNA segment is torsionally unconstrained (referred to as free DNA) or if k_{relax} is very high (where any RNAP-generated supercoiling is quickly relaxed), confirming that the behavior is mediated by the RNAP-generated DNA torsional stress (Figure 2B (inset)).

Next, we simulated the model behavior for increasing values of the RNAP recruitment rate (k_{on}) for a fixed DNA supercoiling relaxation rate (fixed k_{relax}). Computing the average RNAP velocity, we identified three qualitatively distinct regimes of transcription elongation (Figure 2C). In the low k_{on} regime ($k_{on} \lesssim 10^{-2}$ s^{-1}), there is, on average, a single RNAP transcribing the gene at a time, and transcription elongation is the slowest (Figure 2C, D). At higher k_{on} (10^{-2} s$^{-1} < k_{on} < 1$ s^{-1}; shaded region in Figure 2C), we have multiple RNAPs transcribing the gene at the same time. In this regime, cancellation of the RNAP-generated DNA supercoiling between consecutive RNAPs leads to an increase in the average RNAP velocity. At even higher values of k_{on} ($k_{on} > 1$ s^{-1}), the linear density of RNAPs on the gene body saturates (Figure 2D). We refer to this as the 'traffic jam' regime, wherein the trailing RNAPs simply must wait for

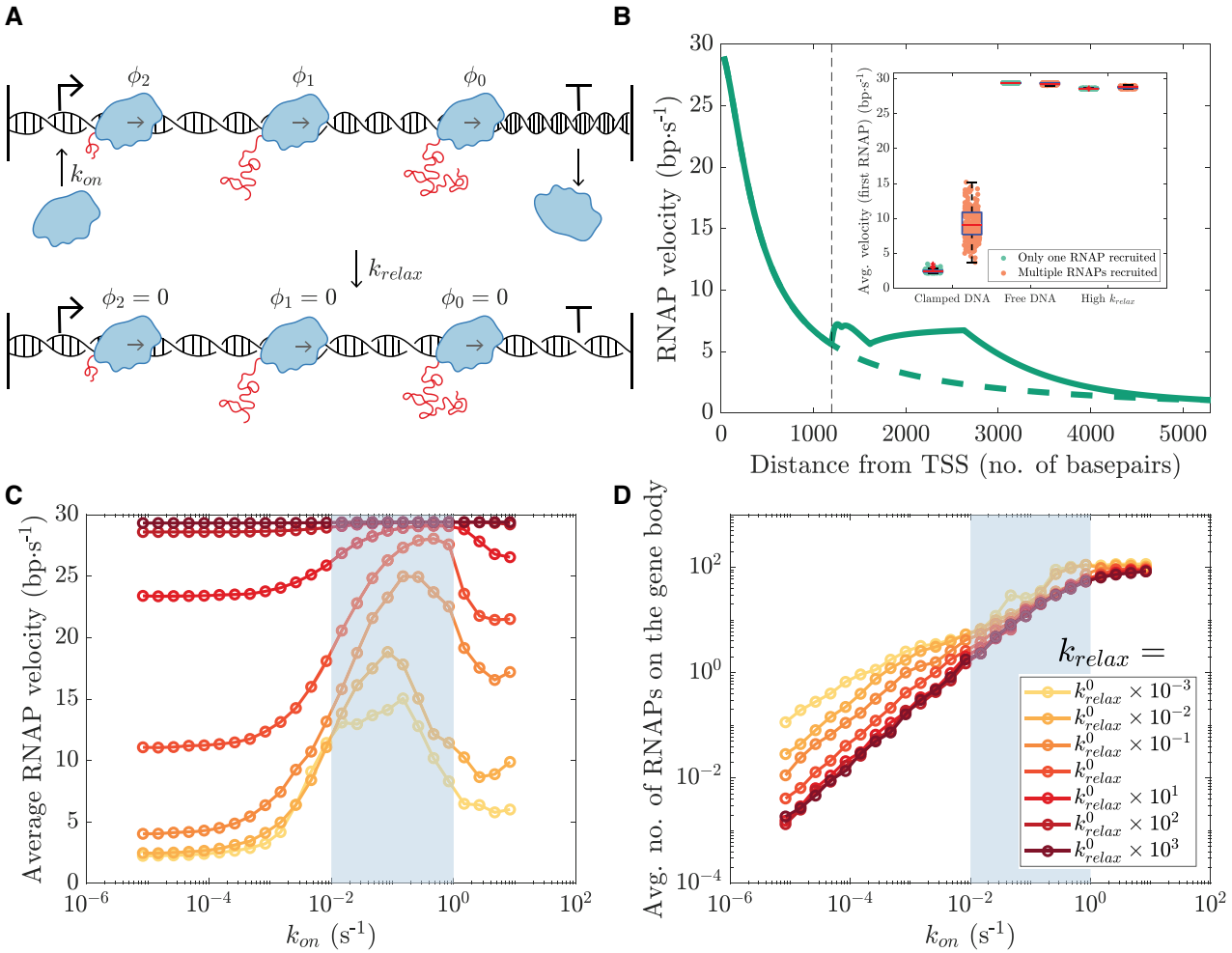

Figure 2. Emergence of DNA supercoiling-mediated collective RNAP behavior. (**A**) In our simulation setup, RNAPs are recruited to the transcription start site at a rate k_{on} and the supercoiling throughout the genomic segment is relaxed at a rate k_{relax}. (**B**) When a second RNAP is recruited to the TSS before the first RNAP has finished transcribing (event indicated by the vertical dashed black line), the translocation rate of the already recruited RNAP increases (shown by the solid green curve). The translocation rate of the first RNAP in the absence of subsequent RNAP recruitment is indicated by the dashed green curve. Inset: when the DNA segment is torsionally constrained (clamped DNA), the velocity of the first RNAP is higher if more RNAPs are subsequently recruited to the same gene. The effect disappears if there is no supercoiling accumulation (torsionally unconstrained or free DNA) or if the RNAP-generated supercoiling is quickly relaxed (high k_{relax}). In each case, the behavior for 256 independent runs is shown. (**C**) The average RNAP velocity varies non-monotonically with k_{on} in the case of torsionally constrained DNA. Collective RNAP behavior, which emerges for $k_{on} > 10^{-2}$ s^{-1} (shaded region), increases the overall transcription elongation rate. However, for very high k_{on} ($k_{on} > 1.0$ s^{-1}), a 'traffic jam'-like scenario decreases the average RNAP velocity. For different transcription initiation rates, the average RNAP velocity increases with the rate of DNA torsional stress relaxation (k_{relax}). (**D**) The average number of co-transcribing RNAPs for different values of k_{on} and k_{relax}. The shaded regions in panels (C) and (D) indicate the range of k_{on} values corresponding to the regime of collective RNAP behavior. Comparison with the case of torsionally unconstrained DNA is shown in Supplementary Figure S7.

the leading RNAP to move forward, resulting in a decrease in the average RNAP translocation rate. The RNAP velocity as a function of the distance from the TSS exhibits qualitatively distinct behaviors in the three regimes (Supplementary Figure S8).

Note that in agreement with previous experimental (2) and theoretical studies (39,40), transcription in our model occurs in bursts (Supplementary Figure S9). Additionally, gene transcription is accompanied by the deposition of positive supercoiling in the DNA downstream of the gene body and negative supercoiling upstream of the TSS (Supplementary Figure S10). The non-monotonic response of the average RNAP velocity to increasing k_{on} is preserved upon varying the different model parameters (Supplementary Figures S11 and S12).

To explore how the rate of DNA torsional stress relaxation affects transcription elongation, we next varied the parameter k_{relax} in our model simulations. Overall, the transcription elongation rate increases with an increase in k_{relax} (Figure 2C). At higher values of k_{relax}, the RNAP-generated DNA supercoils are released more frequently, resulting in lower overall DNA restoring torques on the RNAPs. Higher k_{relax} may thus rescue the poor transcription elongation rates in the low k_{on} regime. At very high value of k_{relax}, the intermediate k_{on} regime involving cooperation between co-transcribing RNAPs disappears. In

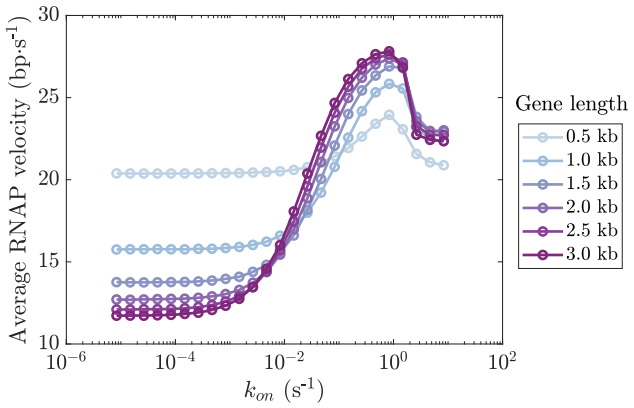

Figure 3. The non-monotonic variation of the average RNAP velocity with the transcription initiation rate is conserved for different gene lengths. While the average RNAP velocity at low k_{on} is lower for longer genes, at higher k_{on}, collective RNAP behavior increases the average RNAP velocity, resulting in higher average velocities in the case of longer genes due to the presence of numerous cooperating RNAPs.

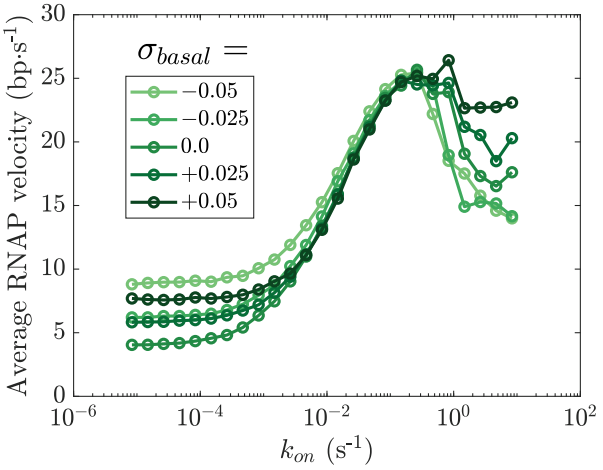

Figure 4. The average transcription elongation rate varies non-monotonically with k_{on} for different values of σ_{basal}. Here, σ_{basal} is the overall supercoiling density in the genomic segment in the absence of any transcription. At low k_{on}, the average RNAP velocity is higher for $|\sigma_{basal}| > 0$. This effect disappears in the RNAP collective behavior regime. Finally, at very high values of k_{on}, the average RNAP velocity is higher if the genomic DNA is maintained in a state with positive basal supercoiling density.

this scenario, DNA supercoiling relaxation by topology manipulation is faster than the rate of RNAP recruitment, and DNA torsional stress is relaxed before it can hinder RNAP movement. The model behavior at very high k_{relax} approaches the behavior in the torsionally unconstrained DNA scenario, thereby confirming the role for DNA torsional stress in the regime characterized by cooperation between co-transcribing RNAPs. Finally, onset of the 'traffic jam' regime described previously is also dependent on k_{relax} (Figure 2C). At higher k_{relax}, the average RNAP velocity is higher. Consequently, the RNAPs spend less time on the gene body, lowering the possibility of a traffic jam. Therefore, increasing k_{relax} shifts the 'traffic jam' regime to higher values of k_{on}.

Longer genes show a wider variation in the transcription elongation rate with k_{on}

In bacteria, genes can vary in length from less than 1 kb to multiple kbps (41). At low values of k_{on}, when there is, on average, a single RNAP transcribing at a time, we observe that the average transcription elongation rate is lower in the case of longer genes (Figure 3). This is because the instantaneous transcription elongation rate for a single RNAP continuously decreases with the distance from the TSS (Figure 1C). Consequently, the overall average transcription elongation rate is lower for longer genes. As we enter the RNAP cooperative behavior regime at higher values of k_{on}, the average elongation rate for longer genes exceeds that for shorter genes. This effect arises from the cancellation of the transcription-mediated DNA supercoiling among the numerous co-transcribing RNAPs in the case of longer genes. Finally, the 'traffic jam'-like regime is largely unaffected by variation in the gene length.

Coexistence of plectonemes or melted DNA with twisted DNA facilitates transcription at low k_{on}

Genomic DNA can be maintained in a twisted or supercoiled state via the sustained activity of DNA topology manipulating motor proteins such as gyrases (34). To investigate how maintaining the DNA in a twisted state will affect transcription elongation, we varied the basal value of the DNA supercoiling density (σ_{basal}) in our simulations. In the updated setup, simulations are started with the genomic DNA with supercoiling density $\sigma_{basal} \neq 0$. Additionally, DNA torsional stress relaxation events in our simulations (occurring at a rate k_{relax}) reset the overall DNA supercoiling density to σ_{basal}. We find that when $|\sigma_{basal}| > 0$, the average transcription elongation rate at low k_{on} is higher than that for the case of $\sigma_{basal} = 0$ (Figure 4). This behavior emerges from the coexistence of plectonemes with unbuckled, twisted DNA for $0.025 \lesssim \sigma \lesssim 0.07$, and from the coexistence of melted DNA with unbuckled DNA for $\sigma \lesssim -0.02$. In these coexistence regimes, change in the supercoiling density shifts the fraction of DNA in the plectonemic, melted, or unbuckled-twisted state while keeping the DNA restoring torque unchanged (23,25,26). During transcription elongation with the DNA in such a coexistence regime, the RNAP experiences net zero DNA restoring torque difference since any RNAP-driven change in σ does not change the DNA torque. For $|\sigma_{basal}| > 0$, a DNA torsional stress relaxation event can put the DNA either inside or close to one of the coexistence regimes. This results in a speed up compared to the scenario with $\sigma_{basal} = 0$ wherein a net DNA restoring torque difference starts building up immediately after a relaxation event. Note that this speed-up disappears for higher values of k_{on} (Figure 4). In the high k_{on} scenario, the DNA supercoiling densities change rapidly as compared to the low k_{on} scenario due to the short DNA segments between the many co-transcribing RNAPs. Consequently, the RNAPs spend only a short period of time in the coexistence regime following a DNA torsional stress relaxation event before the DNA restoring torque difference can start building up again. A non-zero basal supercoiling density thus has little effect on transcription elongation at high k_{on}. Finally, in the 'traffic jam'-like regime at very high

values of k_{on}, the average RNAP velocity is higher for $\sigma_{basal} > 0$ as compared to the $\sigma_{basal} \leq 0$ case.

RNAPs transcribing neighboring genes exhibit DNA supercoiling-mediated coupling

Until now, we have explored how RNAPs co-transcribing the same gene can exhibit collective behavior mediated by the cancellation of DNA twist between co-transcribing RNAPs. In the absence of barriers to supercoiling diffusion between neighboring genes, the same mechanism can also lead to coupling between RNAPs transcribing neighboring genes. Simulating the transcription of two neighboring genes separated by a 'spacer' DNA segment, we find that the coupling between the RNAPs transcribing neighboring genes is dependent on the relative orientation of the neighbors, *i.e.,* whether the genes are in tandem, divergent, or convergent (Figure 5).

If the two genes (gene A and gene B as shown in Figure 5) are in tandem, the negative supercoiling injected into the spacer region by the RNAPs transcribing gene B can be cancelled by the positive supercoiling injected into the spacer during the transcription of gene A. Consequently, turning on gene A speeds up the RNAPs transcribing gene B (Figure 5A), and vice versa (Supplementary Figure S13A). In contrast, when gene A and gene B are in divergent orientation (Figure 5B) or convergent orientation (Figure 5C), their transcription injects the same type of supercoiling into the spacer region (negative supercoiling in the case of divergent genes and positive supercoiling in the case of convergent genes). Therefore, in the divergent and convergent cases, the RNAPs transcribing neighboring genes exhibit mutually repressive behavior: turning gene A off increases the transcription elongation rate for gene B (Figure 5B, C), and vice versa (Supplementary Figure S13B-C).

Interestingly, we find that the effect of transcription of a gene on the transcription elongation rate of the neighboring gene is largely independent of the length of the spacer between the genes (Figure 5 and Supplementary Figure S13). This behavior emerges since the DNA in the spacer region can enter one of the two coexistence regimes—coexistence of twisted, unbuckled DNA with melted DNA (in the case of divergent genes) or with plectonemically buckled DNA (in the case of convergent genes). While the supercoiling density in the spacer region will depend on the length of the spacer region, the DNA restoring torque applied by the spacer will not change with change in the spacer length once the supercoiling density is in one of the coexistence regimes. Note that while the DNA stretching force can alter the regime of coexistence of plectonemes with twisted, unbuckled DNA, the torque-induced melting of DNA is independent of the stretching force (Supplementary Figure S1B). Thus, while the distance independence of the mutual repression in the case of divergent genes will be unaffected by the DNA stretching force, the mutual repression in the case of convergent genes will likely be sensitive to it.

Effect of DNA supercoiling-transcription interplay on RNA production rates

Finally, we investigated the effect of DNA supercoiling on the overall RNA production rate. When k_{on} is high and transcription elongation rather than transcription initiation is the rate limiting step in RNA production, DNA supercoiling-mediated processes can also alter the mean RNA production rate. Consistent with the overall repressive effect of DNA supercoiling on transcription elongation, the mean RNA production rate is higher if the RNAP-generated supercoiling is quickly relaxed (Figure 6A). Similarly, the mean RNA production rate can also be increased by relieving the antagonistic supercoiling being generated from the transcription of a neighboring gene as shown for the case of a convergent gene pair in Figure 6B. Note that for low k_{on}, transcription initiation instead of transcription elongation is the rate-limiting step, and the mean RNA production rate is unaffected by the average RNAP velocity.

Note that in the present study, we do not allow for the premature termination of transcription—RNAPs can dissociate from the gene body only after reaching the transcription termination site. Inclusion of this process into the simulation would likely lower the RNA production rate, especially in the low k_{on} regime wherein the slowly transcribing RNAPs might dissociate from the gene before reaching the end of the gene body.

Biological significance and comparison with experimental data

In bacteria, transcription elongation has long been posited to drive a supercoiling density imbalance between the front and back of an RNAP (1). The resultant torque imbalance, in turn, can affect the rate of RNAP translocation (10). During RNA production, transcription elongation follows transcription initiation, another key step involved in transcription. The question concerning how the transcription elongation rate scales with the transcription initiation rate has long been of interest to both microbiologists and biophysicists (12,21,42).

Recently, Kim *et al.* (3) showed that inhibiting the recruitment of new RNAPs to the transcription start site slows down the already transcribing RNAPs. The same behavior is observed in our model simulations as shown in Figure 2B (inset). Kim *et al.* further showed that the slowdown of already recruited RNAPs disappears if DNA topoisomerase 1 (*topA* gene) is overexpressed. In our model, this behavior is captured upon increasing the DNA torsional stress relaxation rate (k_{relax}). Investigating the dependence of RNAP velocity on the rate of transcription initiation, Kim *et al.* found that decreasing the concentration of a gene inducer over a 20-fold range (thereby decreasing the transcription initiation rate) did not change the average RNAP velocity. When the gene inducer concentration was further decreased by 50-fold, the average RNAP velocity was reduced by one-third. The same trend is observed in our simulations for a parameter subset: when k_{on} is varied within a range ($\sim 0.05-1\ s^{-1}$), the average RNAP velocity does not change appreciably (Figure 2C). This parameter subset corresponds to the biophysical range of transcription initiation rates in bacteria (43). At lower values of k_{on}, we report a significant decrease in RNAP velocity (Figure 2C), once again recapitulating the experimental observations of Kim *et al.* (3). Future studies will test the model predictions in the context of bacterial promoters other than the *lac* promoter (which is the case in (3)).

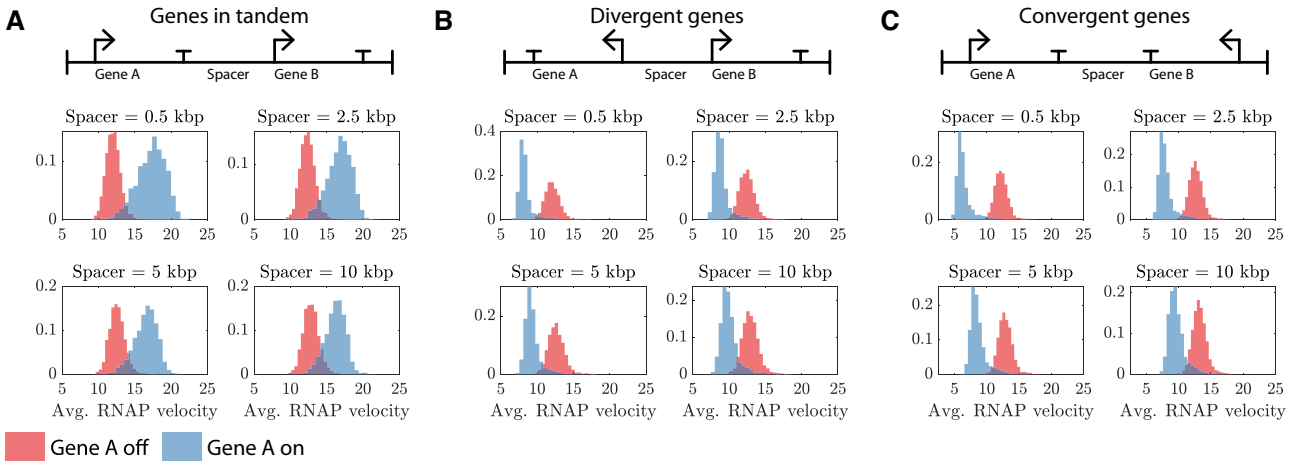

Figure 5. Mechanical coupling between the RNAPs transcribing neighboring genes is dependent on their relative orientation. Each panel shows the distribution of the average velocity of the RNAPs transcribing gene B when gene A is 'off' ($k_{on}^{A} = 0$) and when gene A is 'on' ($k_{on}^{A} = 8.3 \times 10^{-3}$ s^{-1}). The average RNAP velocities are in units of bp·s^{-1}. The histograms in each panel exhibit similar trends despite a 20-fold change in the intergenic distance. kbp: kilo base pairs

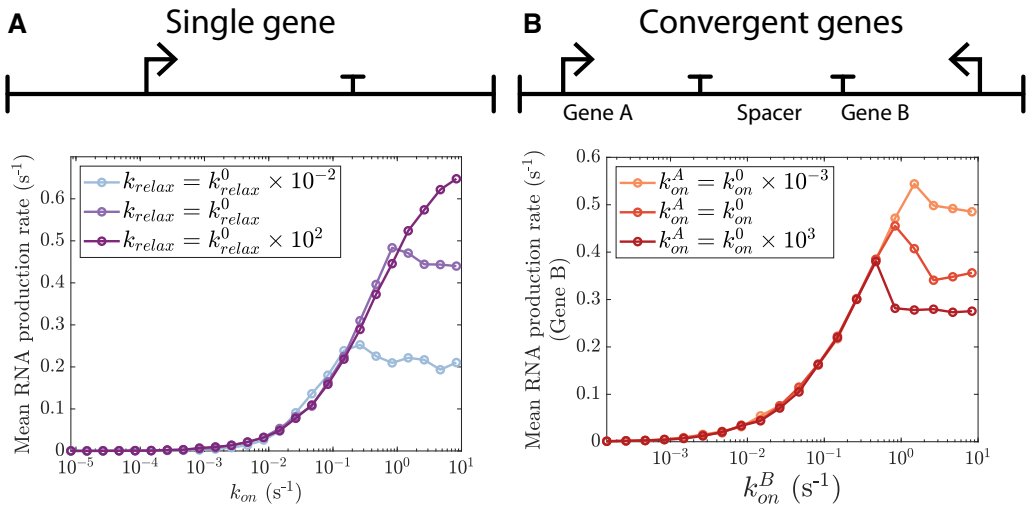

Figure 6. Under high transcription initiation rates, DNA supercoiling-mediated processes can alter the RNA production rates. Here, the mean RNA production rate is the number of RNAPs that finish transcribing per second, on average. (**A**) Rate of RNA production can be increased by quickly relaxing the RNAP-generated supercoiling. Preliminary analysis suggests that the supercoiling relaxation rate can also modulate the shape of the response to a gene inducer (Supplementary Figure S16). (**B**) In a setup with convergent genes, the positive supercoiling injected by gene A slows down the RNA production from gene B provided the transcription initiation rate for gene B is not limiting (k_{on}^{B} is high). The behavior in the case of in tandem and divergent neighbors is shown in Supplementary Figure S14 (also, see Supplementary Figure S15).

A key parameter in our simulation setup is the rate of DNA torsional stress relaxation by enzymes that can manipulate the DNA topology (k_{relax}). This model parameter captures the level of activity of enzymes such as topoisomerases (34,36). We show that the average transcription elongation rate increases monotonically with an increase in k_{relax}. Indeed, DNA torsional stress relaxation by topoisomerases is key to continued transcription in bacteria and inhibitors of these enzymes are potent antibacterial agents (44,45). In the present study, we have used a simplified approach to model the behavior of DNA topology manipulating enzymes. *In vivo*, the activity of such enzymes is a complex process, often involving selective relaxation of a specific type of torsional stress (positive or negative) in discrete steps (46). Incorporating a more biologically detailed model of DNA torsional stress relaxation could be a promising research direction.

Additionally, bacterial gyrases are ATPases and inject negative supercoiling into the genomic DNA to maintain a basal supercoiling density different from the unstressed condition: $\sigma_{basal} \neq 0$ (34,35). In the present study, we have modeled such a scenario by resetting the overall supercoiling density in the genomic segment to $\sigma_{basal} \neq 0$ with every DNA torsional stress relaxation event. For example, the $\sigma_{basal} = -0.025$ curve in Figure 4 corresponds to the scenario wherein gyrase activity maintains the genomic DNA in a negatively supercoiled state. We report that maintaining the DNA in a negatively supercoiled state increases the

RNAP velocity at low k_{on} values. This model behavior is consistent with the decrease in the transcription elongation rates upon gyrase inhibition in bacteria (35). Note that our basic findings concerning the RNAP collective behavior regime are unaffected by a non-zero basal DNA supercoiling density (Figure 4).

Co-regulation of neighboring genes is a well-known paradigm of transcriptional control in bacteria (47–50). Our model suggests that genes oriented in tandem will activate each other, whereas genes in convergent or divergent orientation typically have a mutually repressive effect (Figure 5). Both behaviors, mutual activation in the case of genes oriented in tandem (51) and mutual repression in the case of genes in divergent orientation (3) have been reported in experiments. Our model also recapitulates the experimentally reported accumulation of positive supercoils in the spacer region between convergent genes and that of negative supercoils in the spacer region between divergent genes (3,52,53). Finally, our observation that the supercoiling-mediated interaction between neighboring genes is largely insensitive to the length of spacer DNA between the genes (Figure 5), has also been reported experimentally for the case of genes in tandem (51) and for divergent genes (3).

DISCUSSION

The DNA supercoiling-transcription interplay has been of interest for several decades (54), with recent experimental advances revealing the microscopic details (2–3,5,51,55,56). Here, we have described a framework for transcription elongation that, unlike previously posited theoretical models (12,13,15–17), incorporates precise mechanical properties of DNA including plectoneme formation. The model builds upon the torque-balance description put forth by Sevier and Levine (14) while adding an experimental data-informed choice of RNAP velocity dependence on the net DNA restoring torque. A recent study incorporates a similar dependence of RNAP velocity on the DNA restoring torque difference while relying on a more phenomenological description of DNA restoring torque as a function of the RNAP count on the gene body (18). A key result of our modeling study is that cancellation and equilibration of RNAP-generated DNA torsional stress is sufficient to drive coupling between co-transcribing RNAPs. Our model recapitulates the DNA torsion-mediated collective behavior of co-transcribing RNAPs and makes multiple verifiable predictions— non-monotonic variation of the transcription elongation rate with transcription initiation (Figure 2C), and dependence of the transcription elongation rate on different biologically relevant parameters, including gene length (Figure 3) and the basal DNA supercoiling density (Figure 4).

The results presented in this study rely on two key hypotheses. First, RNAP translocation injects negative supercoiling into the upstream DNA and positive supercoiling into the downstream DNA. This DNA twisting by the RNAP results in a DNA restoring torque which depends on the level of supercoiling injected into the DNA (as shown in Supplementary Figure S1). Second, a net positive torque difference across the RNAP decreases the rate of RNAP translocation (reported by Ma *et al.* (10); Figure 1B). In the presence of multiple co-transcribing RNAPs, the RNAP-injected supercoiling can be cancelled out among the adjacent RNAPs, speeding up the transcription elongation process and resulting in the emergence of a collective behavior regime (Figure 2B, C). The DNA supercoiling-dependence of RNAP translocation additionally results in transcription dependence on cellular processes that can manipulate the DNA topology (Figure 4) and on the status of neighboring genes (Figures 5, 6B, and Supplementary Figure S14).

Understanding how DNA supercoiling affects transcription could be key to progress in synthetic biology when it comes to designing gene constructs that exhibit predictable gene expression patterns (49,57). Our model shows that the rate of RNA production can depend on topoisomerase activity—variation in topoisomerase activity from cell to cell could therefore be a driver of heterogeneity in gene expression. Preliminary analysis (shown in Supplementary Figure S16) further suggests that the topoisomerase activity can also modulate the shape of the response to a gene inducer. Our model can be helpful in guiding the design of synthetic circuits utilizing supercoiling-related processes to one's advantage.

Note that in the present study, we have assumed that the transcription initiation rate is independent of the supercoiling density at the promoter site. There have been multiple experimental reports indicating that the transcription initiation rate is higher if the promoter DNA is negatively twisted (55,58–60). This dependence has been modeled using phenomenological approaches such as a sigmoidal dependence (16), a linear dependence (13,17), and a more complex relation based on the free energy of transcription bubble-formation (15). Introducing a supercoiling-sensitive k_{on} in our model will likely introduce a positive feedback into the transcriptional process since the promoter site in our model becomes negatively supercoiled when the gene is under transcription. We note that while Kim *et al.* have shown that divergent genes repress each other (3), others have indicated the possibility of mutual activation between the genes in such a pair (56,61). Once a supercoiling-dependent k_{on} is included in the modeling framework, competition between the mutually activating effects mediated by the deposition of negative supercoiling in the spacer region and the mutually repressive effects driven by the DNA restoring torque will likely lead to a more complex, context-sensitive behavior in the specific case of divergent genes. Incorporation of the supercoiling density-dependence of transcription initiation will thus be an interesting and useful extension of the present model. Such an extension would also be helpful in understanding the role of DNA supercoiling in mediating the bacterial response to stress or nutrient deprivation (62,63).

We further note that the present model assumes the DNA torsional response to be instantaneous. This is a good approximation for the case of twist relaxation. However, the writhe dynamics of DNA is rather slow (64,65). The differing twist and writhe relaxation time scales could imply that DNA topology relaxation events *in vivo* dissipate more twist than writhe. The present model also does not account for features like plectoneme-domain multiplicity (31), dependence of DNA mechanical properties (66) and melting energy (67) on the nucleotide sequence, or for the

hindrance of RNAP movement by slowly diffusing plectoneme domains. The recent simulation-based finding that transcription-generated plectonemes are formed far away from the RNAPs, however, suggests that hindrance by plectonemes is unlikely to substantially interfere with transcription elongation (65).

The present model is limited to the DNA supercoiling-transcription interplay in prokaryotes. In eukaryotes, the genomic DNA is wrapped around histones which change the linking number of DNA by introducing writhe (68). Transcription elongation in eukaryotes proceeds with the expulsion of histones which may be facilitated by the torsional stress introduced by an RNAP (69). Moreover, histones can serve as a buffer for the positive twist injected into the downstream DNA (70). Incorporating these effects will be key to understanding the supercoiling-transcription interplay in eukaryotes as well as the role of supercoiling in chromatin organization (9,71).

SUPPLEMENTARY DATA

Supplementary Data are available at NAR Online.

FUNDING

National Science Foundation [PHY-2019745, CHE-1614101]; Welch Foundation [C-1792]; J.N.O. is a Cancer Prevention and Research Institute of Texas (CPRIT) Scholar in Cancer Research. Funding for open access charge: National Science Foundation [PHY-2019745].
Conflict of interest statement. None declared.

REFERENCES

1. Liu,L.F. and Wang,J.C. (1987) Supercoiling of the DNA template during transcription. *Proc. Natl. Acad. Sci. U.S.A.*, **84**, 7024–7027.
2. Chong,S., Chen,C., Ge,H. and Xie,X.S. (2014) Mechanism of transcriptional bursting in bacteria. *Cell*, **158**, 314–326.
3. Kim,S., Beltran,B., Irnov,I. and Jacobs-Wagner,C. (2019) Long-distance cooperative and antagonistic RNA polymerase dynamics via DNA supercoiling. *Cell*, **179**, 106–119.
4. Postow,L., Hardy,C.D., Arsuaga,J. and Cozzarelli,N.R. (2004) Topological domain structure of the *Escherichia coli* chromosome. *Genes Dev.*, **18**, 1766–1779.
5. Le,T. B.K., Imakaev,M.V., Mirny,L.A. and Laub,M.T. (2013) High-resolution mapping of the spatial organization of a bacterial chromosome. *Science*, **342**, 731–734.
6. Le,T.B.K. and Laub,M.T. (2016) Transcription rate and transcript length drive formation of chromosomal interaction domain boundaries. *EMBO J.*, **35**, 1582–1595.
7. Gilbert,N. and Allan,J. (2014) Supercoiling in DNA and chromatin. *Curr. Opin. Genet. Dev.*, **25**, 15–21.
8. Racko,D., Benedetti,F., Dorier,J. and Stasiak,A. (2018) Are TADs supercoiled? *Nucleic Acids Res.*, **47**, 521–532.
9. Neguembor,M.V., Martin,L., Álvaro,C.-G., Gómez-García,P.A., Vicario,C., Carnevali,D., AlHaj Abed,J., Granados,A., Sebastian-Perez,R., Sottile,F. *et al.* (2021) Transcription-mediated supercoiling regulates genome folding and loop formation. *Mol. Cell*, **81**, 3065–3081.
10. Ma,J., Bai,L. and Wang,M.D. (2013) Transcription under torsion. *Science*, **340**, 1580–1583.
11. Forde,N.R., Izhaky,D., Woodcock,G.R., Wuite,G.J.L. and Bustamante,C. (2002) Using mechanical force to probe the mechanism of pausing and arrest during continuous elongation by Escherichia coli RNA polymerase. *Proc. Natl. Acad. Sci. U.S.A.*, **99**, 11682–11687.
12. Heberling,T., Davis,L., Gedeon,J., Morgan,C. and Gedeon,T. (2016) A mechanistic model for cooperative behavior of co-transcribing RNA polymerases. *PLoS Comput. Biol.*, **12**, e1005069.
13. Brackley,C.A., Johnson,J., Bentivoglio,A., Corless,S., Gilbert,N., Gonnella,G. and Marenduzzo,D. (2016) Stochastic model of supercoiling-dependent transcription. *Phys. Rev. Lett.*, **117**, 018101.
14. Sevier,S.A. and Levine,H. (2018) Properties of gene expression and chromatin structure with mechanically regulated elongation. *Nucleic Acids Res.*, **46**, 5924–5934.
15. Meyer,S. and Beslon,G. (2014) Torsion-mediated interaction between adjacent genes. *PLoS Comput. Biol.*, **10**, e1003785.
16. El Houdaigui,B., Forquet,R., Hindré,T., Schneider,D., Nasser,W., Reverchon,S. and Meyer,S. (2019) Bacterial genome architecture shapes global transcriptional regulation by DNA supercoiling. *Nucleic Acids Res.*, **47**, 5648–5657.
17. Ancona,M., Bentivoglio,A., Brackley,C.A., Gonnella,G. and Marenduzzo,D. (2019) Transcriptional bursts in a nonequilibrium model for gene regulation by supercoiling. *Biophys. J.*, **117**, 369–376.
18. Chatterjee,P., Goldenfeld,N. and Kim,S. (2021) DNA supercoiling drives a transition between collective modes of gene synthesis. *Phys. Rev. Lett.*, **127**, 218101.
19. Borukhov,S. and Nudler,E. (2008) RNA polymerase: the vehicle of transcription. *Trends Microbiol.*, **16**, 126–134.
20. Le,T.T. and Wang,M.D. (2018) Molecular highways—navigating collisions of DNA motor proteins. *J. Mol. Biol.*, **430**, 4513–4524.
21. Epshtein,V. and Nudler,E. (2003) Cooperation between RNA polymerase molecules in transcription elongation. *Science*, **300**, 801–805.
22. Costa,P.R., Acencio,M.L. and Lemke,N. (2013) Cooperative RNA polymerase molecules behavior on a stochastic sequence-dependent model for transcription elongation. *PLoS One*, **8**, e57328.
23. Marko,J.F. (2007) Torque and dynamics of linking number relaxation in stretched supercoiled DNA. *Phys. Rev. E*, **76**, 021926.
24. Marko,J.F. and Neukirch,S. (2012) Competition between curls and plectonemes near the buckling transition of stretched supercoiled DNA. *Phys. Rev. E*, **85**, 011908.
25. Marko,J.F. and Neukirch,S. (2013) Global force-torque phase diagram for the DNA double helix: Structural transitions, triple points, and collapsed plectonemes. *Phys. Rev. E*, **88**, 062722.
26. Meng,H., Bosman,J., van der Heijden,T. and van Noort,J. (2014) Coexistence of twisted, plectonemic, and melted DNA in small ropological domains. *Biophys. J.*, **106**, 1174–1181.
27. Marko,J.F. (2015) Biophysics of protein–DNA interactions and chromosome organization. *Physica A*, **418**, 126–153.
28. Dillon,S.C. and Dorman,C.J. (2010) Bacterial nucleoid-associated proteins, nucleoid structure and gene expression. *Nat. Rev. Microbiol.*, **8**, 185–195.
29. Leng,F., Chen,B. and Dunlap,D.D. (2011) Dividing a supercoiled DNA molecule into two independent topological domains. *Proc. Natl. Acad. Sci. U.S.A.*, **108**, 19973–19978.
30. Milo,R., Jorgensen,P., Moran,U., Weber,G. and Springer,M. (2010) BioNumbers—the database of key numbers in molecular and cell biology. *Nucleic Acids Res.*, **38**, D750–D753.
31. Brahmachari,S., Dittmore,A., Takagi,Y., Neuman,K.C. and Marko,J.F. (2018) Defect-facilitated buckling in supercoiled double-helix DNA. *Phys. Rev. E*, **97**, 022416.
32. Strick,T., Allemand,J.-F., Croquette,V. and Bensimon,D. (2000) Twisting and stretching single DNA molecules. *Prog. Biophys. Mol. Biol.*, **74**, 115–140.
33. Herzel,L., Ottoz,D.S., Alpert,T. and Neugebauer,K.M. (2017) Splicing and transcription touch base: co-transcriptional spliceosome assembly and function. *Nat. Rev. Mol. Cell Biol.*, **18**, 637–650.
34. Zechiedrich,E.L., Khodursky,A.B., Bachellier,S., Schneider,R., Chen,D., Lilley,D. M.J. and Cozzarelli,N.R. (2000) Roles of topoisomerases in maintaining steady-state DNA supercoiling in Escherichia coli. *J. Biol. Chem.*, **275**, 8103–8113.
35. Rovinskiy,N., Agbleke,A.A., Chesnokova,O., Pang,Z. and Higgins,N.P. (2012) Rates of gyrase supercoiling and transcription elongation control supercoil density in a bacterial chromosome. *PLoS Genet.*, **8**, e1002845.
36. Bush,N.G., Evans-Roberts,K., Maxwell,A. and Lovett,S.T. (2015) DNA topoisomerases. *EcoSal Plus*, **6**, https://doi.org/10.1128/ecosalplus.ESP-0010-2014.

37. Sevier,S.A. (2020) Mechanical properties of DNA replication. *Phys. Rev. Research*, **2**, 023280.
38. Gillespie,D.T. (1977) Exact stochastic simulation of coupled chemical reactions. *J. Phys. Chem.*, **81**, 2340–2361.
39. Sevier,S.A., Kessler,D.A. and Levine,H. (2016) Mechanical bounds to transcriptional noise. *Proc. Natl. Acad. Sci. U.S.A.*, **113**, 13983–13988.
40. Klindziuk,A., Meadowcroft,B. and Kolomeisky,A.B. (2020) A mechanochemical model of transcriptional bursting. *Biophys. J.*, **118**, 1213–1220.
41. Xu,L., Chen,H., Hu,X., Zhang,R., Zhang,Z. and Luo,Z.W. (2006) Average gene length is highly conserved in prokaryotes and eukaryotes and diverges only between the two kingdoms. *Mol. Biol. Evol.*, **23**, 1107–1108.
42. Saeki,H. and Svejstrup,J.Q. (2009) Stability, flexibility, and dynamic interactions of colliding RNA polymerase II elongation complexes. *Mol. Cell*, **35**, 191–205.
43. Bremer,H. and Dennis,P.P. (1996) Modulation of chemical composition and other parameters of the cell by growth rate. In: Neidhardt,F.C., Curtiss,R., Ingraham,J.L., Lin,E.C.C., Low,K.B., Magasanik,B., Reznikoff,W.S., Riley,M., Schaechter,M. and Umbarger,H.E. (eds). *Escherichia coli and Salmonella: Cellular and Molecular Biology*. 2nd edn. ASM Press, Washington, DC, pp. 1553–1569.
44. Maxwell,A. (1997) DNA gyrase as a drug target. *Trends Microbiol.*, **5**, 102–109.
45. Hiasa,H. (2017) DNA topoisomerases as targets for antibacterial agents. In: Drolet,M. (ed). *DNA Topoisomerases, Vol. 1703 of Methods in Molecular Biology*. Humana Press, NY, pp. 47–62.
46. Baranello,L., Wojtowicz,D., Cui,K., Devaiah,B., Chung,H.-J., Chan-Salis,K., Guha,R., Wilson,K., Zhang,X., Zhang,H. *et al.* (2016) RNA polymerase II regulates topoisomerase 1 activity to favor efficient transcription. *Cell*, **165**, 357–371.
47. Korbel,J.O., Jensen,L.J., Von Mering,C. and Bork,P. (2004) Analysis of genomic context: prediction of functional associations from conserved bidirectionally transcribed gene pairs. *Nat. Biotechnol.*, **22**, 911–917.
48. Brophy,J. A.N. and Voigt,C.A. (2016) Antisense transcription as a tool to tune gene expression. *Mol. Syst. Biol.*, **12**, 854.
49. Yeung,E., Dy,A.J., Martin,K.B., Ng,A.H., Del Vecchio,D., Beck,J.L., Collins,J.J. and Murray,R.M. (2017) Biophysical constraints arising from compositional context in synthetic gene networks. *Cell Syst.*, **5**, 11–24.
50. Pannier,L., Merino,E., Marchal,K. and Collado-Vides,J. (2017) Effect of genomic distance on coexpression of coregulated genes in *E. coli*. *PLoS One*, **12**, e0174887.
51. Moulin,L., Rahmouni,A.R. and Boccard,F. (2005) Topological insulators inhibit diffusion of transcription-induced positive supercoils in the chromosome of *Escherichia coli*. *Molecular Microbiology*, **55**, 601–610.
52. Guo,M.S., Kawamura,R., Littlehale,M.L., Marko,J.F. and Laub,M.T. (2021) High-resolution, genome-wide mapping of positive supercoiling in chromosomes. *eLife*, **10**, e67236.
53. Pannunzio,N. and Lieber,M. (2016) Dissecting the roles of divergent and convergent transcription in chromosome instability. *Cell Rep.*, **14**, 1025–1031.
54. Dorman,C.J. (2019) DNA supercoiling and transcription in bacteria: a two-way street. *BMC Mol. Cell Biol.*, **20**, 26.
55. Ouafa,Z.-A., Reverchon,S., Lautier,T., Muskhelishvili,G. and Nasser,W. (2012) The nucleoid-associated proteins H-NS and FIS modulate the DNA supercoiling response of the pel genes, the major virulence factors in the plant pathogen bacterium Dickeya dadantii. *Nucleic Acids Res.*, **40**, 4306–4319.
56. Eszterhas,S.K., Bouhassira,E.E., Martin,D.I.K. and Fiering,S. (2002) Transcriptional interference by independently regulated genes occurs in any relative arrangement of the genes and is influenced by chromosomal integration position. *Mol. Cell Biol.*, **22**, 469–479.
57. Cardinale,S. and Arkin,A.P. (2012) Contextualizing context for synthetic biology – identifying causes of failure of synthetic biological systems. *Biotechnol. J.*, **7**, 856–866.
58. Wood,D.C. and Lebowitz,J. (1984) Effect of supercoiling on the abortive initiation kinetics of the RNA-I promoter of ColE1 plasmid DNA. *J. Biol. Chem.*, **259**, 11184–11187.
59. Borowiec,J.A. and Gralla,J.D. (1985) Supercoiling response of the lac ps promoter in vitro. *J. Mol. Biol.*, **184**, 587–598.
60. Buc,H. and McClure,W.R. (1985) Kinetics of open complex formation between *Escherichia coli* RNA polymerase and the lac UV5 promoter. Evidence for a sequential mechanism involving three steps. *Biochemistry*, **24**, 2712–2723.
61. Sobetzko,P. (2016) Transcription-coupled DNA supercoiling dictates the chromosomal arrangement of bacterial genes. *Nucleic Acids Res.*, **44**, 1514–1524.
62. Bordes,P., Conter,A., Morales,V., Bouvier,J., Kolb,A. and Gutierrez,C. (2003) DNA supercoiling contributes to disconnect σ^S accumulation from σ^S-dependent transcription in Escherichia coli. *Mol. Microbiol.*, **48**, 561–571.
63. Blot,N., Mavathur,R., Geertz,M., Travers,A. and Muskhelishvili,G. (2006) Homeostatic regulation of supercoiling sensitivity coordinates transcription of the bacterial genome. *EMBO Rep.*, **7**, 710–715.
64. van Loenhout,M. T.J., de Grunt,M.V. and Dekker,C. (2012) Dynamics of DNA supercoils. *Science*, **338**, 94–97.
65. Fosado,Y.A.G., Michieletto,D., Brackley,C.A. and Marenduzzo,D. (2021) Nonequilibrium dynamics and action at a distance in transcriptionally driven DNA supercoiling. *Proc. Natl. Acad. Sci. U.S.A.*, **118**, e1905215118.
66. Rief,M., Clausen-Schaumann,H. and Gaub,H.E. (1999) Sequence-dependent mechanics of single DNA molecules. *Nat. Struct. Mol. Biol.*, **6**, 346–349.
67. Vlijm,R. V.D., Torre,J. and Dekker,C. (2015) Counterintuitive DNA sequence dependence in supercoiling-induced DNA melting. *PLoS One*, **10**, e0141576.
68. Kouzine,F., Sanford,S., Elisha-Feil,Z. and Levens,D. (2008) The functional response of upstream DNA to dynamic supercoiling in vivo. *Nat. Struct. Mol. Biol.*, **15**, 146.
69. Teves,S.S. and Henikoff,S. (2014) Transcription-generated torsional stress destabilizes nucleosomes. *Nat. Struct. Mol. Biol.*, **21**, 88–94.
70. Kaczmarczyk,A., Meng,H., Ordu,O., van Noort,J. and Dekker,N.H. (2020) Chromatin fibers stabilize nucleosomes under torsional stress. *Nat. Commun.*, **11**, 126.
71. Naughton,C., Avlonitis,N., Corless,S., Prendergast,J.G., Mati,I.K., Eijk,P.P., Cockroft,S.L., Bradley,M., Ylstra,B. and Gilbert,N. (2013) Transcription forms and remodels supercoiling domains unfolding large-scale chromatin structures. *Nat. Struct. Mol. Biol.*, **20**, 387.